FULL TITLE
ASP Conference Series, Vol. **VOLUME**, **YEAR OF PUBLICATION**
NAMES OF EDITORS

Spectropolarimetric diagnostics at the solar photosphere near the limb

L. Yelles Chaouche, S. K. Solanki

Max Planck Institut für Sonnensystemforshung, Max-Planck-strasse,2, Katlenburg-Lindau 37191, Germany

L. Rouppe van der Voort and M. van Noort

Institute of Theoretical Astrophysics, P.O. box 1029 Blindern N-0315, Oslo, Norway

Abstract. In the present work, we investigate the formation of Stokes profiles and spectro-polarimetric diagnostics in an active region plage near the limb. We use 3-D radiation-MHD simulations with unipolar fields of an average strength of 400G, which is largely concentrated in flux tubes in which the field reaches typical kilo-Gauss values. We generate synthetic Stokes spectra by radiative transfer calculations, then we degrade the simulated Stokes signal to account for observational conditions. The synthetic data treated in this manner are compared with and found to roughly reproduce spectro-polarimetric high-resolution observations at μ=0.39 obtained by the SOUP instrument with the Swedish 1-m Solar Telescope at the beginning of 2006.

1. Introduction

The study of small scale magnetic flux concentrations near the solar limb provides additional insight into the existing models of magnetic flux concentrations (Frutiger et al. 2003). These flux concentrations have been associated with solar faculae. Understanding the physical processes behind solar faculae through observations and simulations is an important topic (Lites et al. 2004; Keller et al. 2004; Carlsson et al. 2004; Steiner 2005; Hirzberger & Wiehr 2005; Okunev & Kneer 2005; De Pontieu et al. 2006). One of the motivations for studying the facular phenomenon is the influence of their brightness on the Sun's irradiance variation (Fligge & Solanki 2001).

In order to gain further insight into magnetic flux concentrations in plage regions at intermediate μ values, we perform a study of the spectropolarimetric signal in MHD simulations and observations originating from plage regions at $\mu = 0.39$. The simulations used here are fully compressible 3-D radiation-MHD simulations (Vögler & Schüssler 2003; Vögler et al. 2005). The observations has been recorded with the SOUP instrument (Title & Rosenberg 1981) at the Swedish 1-m Solar Telescope (SST) in 2006.

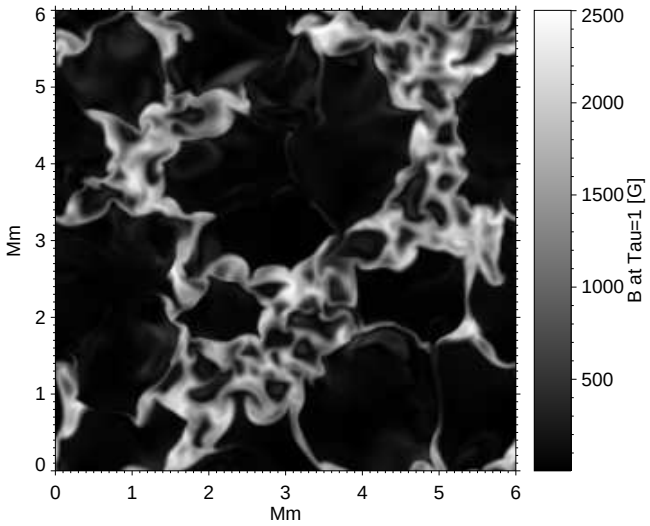

Figure 1. Magnetic field strength map at an optical depth $\tau_{5000} = 1$.

2. Methods and simulations

The 3D radiation-MHD simulations used include, a solution of the fully compressible MHD equations, including partial ionization in the equation of state and a non-local non-grey radiative transfer (Vögler & Schüssler 2003; Vögler et al. 2005). The MHD simulation box is 6x6 Mm in the horizontal plane and 1.4 Mm in the vertical direction, with a resolution of 288x288x100 grid points. The mean magnetic field strength is about 400 G. (See Figures 1 and 2). In these Figures we can see the fully developed granulation pattern which has interacted with the magnetic field. The flux gets concentrated in intergranular lanes as a result of flux expulsion (Schüssler 1990). The flux concentrations appear darker than the average granular intensity. This is due to the partially suppressed plasma motion through field lines. Nevertheless, a proper analysis of energy exchange via convection and radiation is necessary before drawing conclusions on the thermal, and radiative properties of flux concentrations (Schüssler et al. 2003). This is beyond the scope of the present paper.

We construct an inclined view of the simulation box by interpolation of the different quantities along rays with the desired inclination angle. This allows comparisons with observations away from disk center. Fig. 3 shows an inclined view of Fig. 2 at an angle of 67 degrees ($\mu = 0.39$). One can notice the higher values of intensity at some locations (e.g. at coordinates (2200km, 300km) and (3000km, 600km)). These are identified as faculae (Keller et al. 2004).

In order to compare these 3D radiative-MHD simulations with Spectropolarimetric observations, we have to calculate the Stokes signal emerging from the inclined simulation box (e.g. the continuum intensity map near 6302.5 Å is shown in Figure 3). This is done using the STOPRO code in the SPINOR package (Solanki 1987; Frutiger et al. 2000). In order to take into account ef-

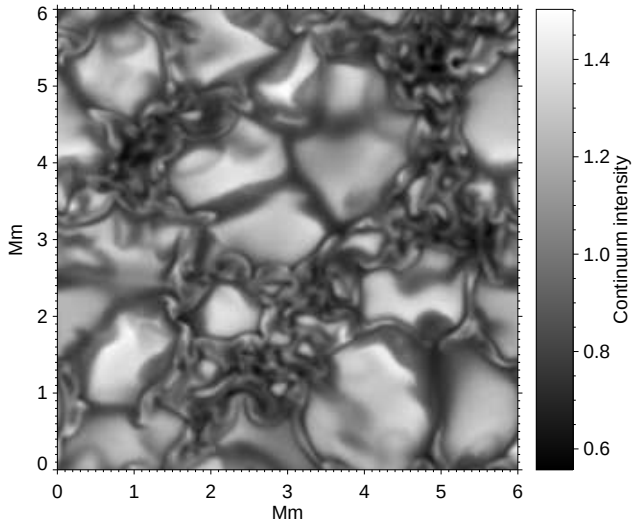

Figure 2. Normalized continuum intensity map near 6302.5 Å emerging from the simulation box at disc center.

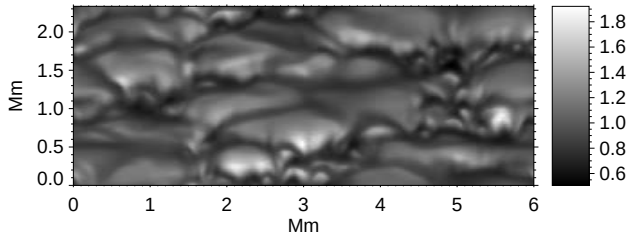

Figure 3. Normalized continuum intensity map near 6302.5 Å emerging from the simulation box at $\mu = 0.39$.

fects such as the finite aperture of the telescope, and seeing, we perform then a spectral and spatial smearing of these synthetic polarimetric data.

3. Comparison with spectropolarimetric observations at Mu=0.39

We compare the emerging Stokes signal from the simulation run with a set of high spatial resolution spectropolarimetric images obtained with the SOUP instrument at the Swedish 1-m Solar Telescope. The observational data consists of 9 images: the four Stokes polarization images at both + and -50 mÅ from the line center of the Fe I 6302.5 Å line, and a wide band image. The images are restored using the Multi-Object Multi-Frame Blind Deconvolution (MOMFBD) image restoration method (van Noort et al. 2005). The SOUP images are based on 480 exposures at each line position which means that the effective exposure time amounts to 7.2 s. The combined use of the SST adaptive optics system

and MOMFBD post-processing resulted in a spatial resolution in the Stokes observations that approaches the diffraction limit of the telescope (better than 0.2 arcsec). In order to find the actual resolution of the polarimetric observations, we carry out the following steps: 1/ We choose a quiet-sun simulation run and convolve the synthetic Stokes profiles in the spectral dimension with a Lyot type filter of FWHM=70 mÅ (similar to SOUP). 2/ In order to account for the lower spatial resolution in the observations, we apply a low-pass filter to the synthetic images which has the shape of a top-hat function and effectively removes power at the highest spatial frequencies - beyond the spatial resolution of the observations. In addition, we convolve the synthetic images with a Lorentzian profile which accounts for the far wings of the PSF that are not corrected for in the MOMFBD restoration. 3/ We pick a quiet region from the observed Stokes-I images either at + 50 mÅ or -50 mÅ and compare it with the synthetic ones. The matching of the two data sets is done by comparing their power spectra (Figure 4 upper panel) and their standard deviations. This is done through an iterative process where both the FWHM of the PSF and Lorenz profile are allowed to change until the two data-sets fit with each other.

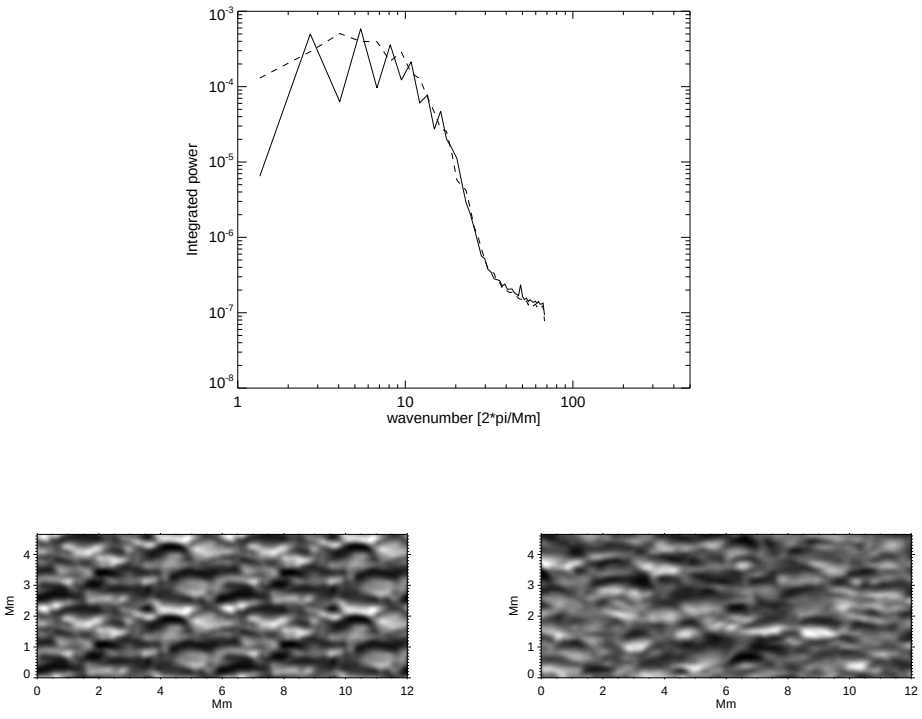

Figure 4. Two lower panels: Stokes-I maps at +50 mÅ from line center Fe I 6302.5 Å. Lower left: simulations, lower right : observations. The upper panel shows the integrated power spectra for the two lower images (full line : observations, dashed line: simulations).

The so obtained degrading parameters are used when comparing more active regions, like the ones in Figure 5. The two lower panels of Figure 4 indicate the

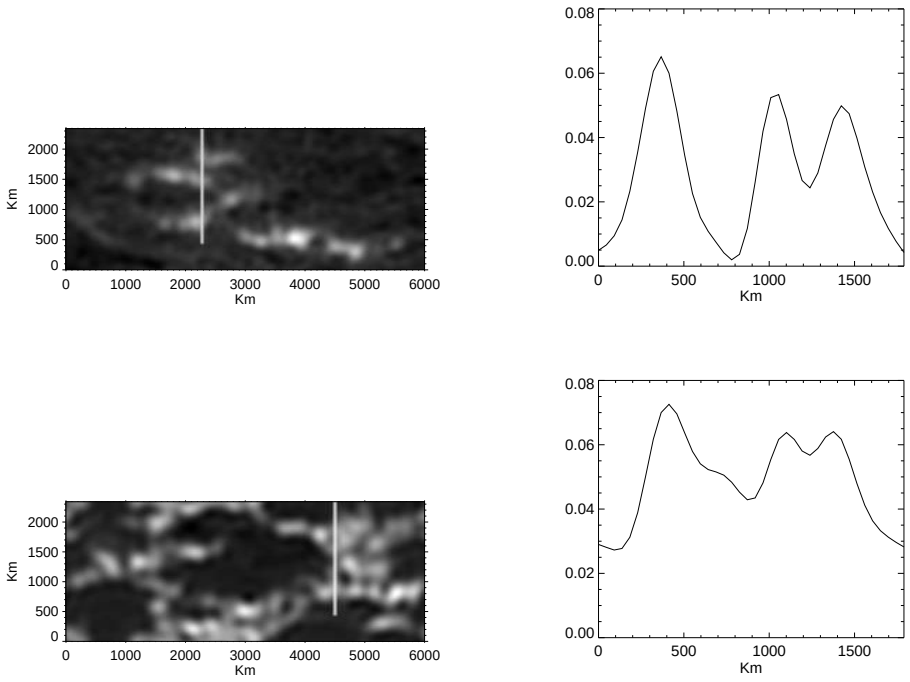

Figure 5. Upper left panel: observed Stokes-V at -50 mÅ from line center Fe I 6302.5 Å. Lower left panel: Stokes-V from simulations degraded to the resolution of observations. A measure of the Stokes-V signal at the white slits-positions is shown on the right panels.

observed (right one) and degraded-simulated (left one) Stokes-I maps at +50 mÅ from line center (Fe I 6302.5 Å). The simulated map corresponds to a quiet region where the mean field strength is about 20G. One can see the similarity of the two images. The original observed image was inclined by an angle of about 20 degrees, which we have corrected here.

In the two left images in Figure 5, we see an observations and a degraded simulation of Stokes-V at -50 mÅ. A direct quantitative comparison between Stokes-V signals in these two images can be done by plotting the signal along slits (e.g. the white slits in the left panels). The resulting signal is shown in the two right panels. We observe that the two curves are reasonably similar. This indicates that the observed features here are well reproduced by an MHD simulation run with an average field strength of 400G. At this stage we can address the question: does the MHD simulation-run reproduce the actual photospheric situation at the observed region on figure 5 ?. The results above are in favor of a positive answer. But the fact that we have only two spectral positions at +50 mÅ and -50 mÅ makes it necessary to proceed to further comparisons with a larger spectral sampling. Then, in case simulations and observations match, we can proceed further by studying these regions in detail directly from the MHD simulations.

4. Conclusions

We presented here a comparative study about small-scale magnetic flux concentrations near the solar limb. This is part of a more general work aiming at investigating their physical and spectropolrimetric properties through Stokes-diagnostics and direct MHD simulations. We focussed here on identifying similarities between observed and simulated Stokes signal at + and -50 mÅ from line center of Fe I 6302.5 Å. The comparison has been made possible, by introducing suitable instrumental and seeing degradation to the simulated Stokes signal. We thus identified similarities between the observed and simulated maps of Stokes-V at two wavelength positions + and -50 mÅ from line center of Fe I 6302.5 Å. Although we see similarities, we mention the necessity of further investigation before concluding that the simulations are indeed reproducing the observed magnetic features. Such investigations should include more spectral positions, allowing a more consistent study of the variation of physical quantities (e.g. temperature, magnetic field vector, line-of-sight velocity) through the inclined magnetic flux concentrations.

References

Carlsson, Mats, Stein, Robert F., Nordlund, Åke & Scharmer, Gran B. 2004, ApJ, 610L, 137

De Pontieu, B.; Carlsson, M.; Stein, R.; Rouppe van der Voort, L.; Lfdahl, M.; van Noort, M.; Nordlund, .; Scharmer, G. 2006, ApJ, 646, 1405

Fligge, M. & Solanki, S. K. 2001, Astronomical and Astrophysical Transactions, 20, 467

Frutiger, C.; Solanki, S. K.; Fligge, M.; Bruls, J. H. M. J. 2000, A&A, 358, 1109

Frutiger, C., Solanki, S. K. & Gandorfer, A. 2003, ASPC, 307, 344

Hirzberger, J. & Wiehr, E. 2005, A&A, 438, 1059

Keller, C. U., Schüssler, M., Vögler, A. & Zakharov, V. 2004, ApJ, 607L, 59

Lites, B. W., Scharmer, G. B., Berger, T. E. & Title, A. M. 2004, Solar Physics, 221, 65

Okunev, O. V. & Kneer, F. 2005, A&A, 439, 323

Schüssler, M. 1990, IAUS, 138, 161

Schüssler, M.; Shelyag, S.; Berdyugina, S.; Vögler, A.; Solanki, S. K. 2003, ApJ, 597L, 173

Solanki, S. K. 1987, PhD Thesis (ETH Zürich)

Spruit, H. C. 1979, Solar Physics, 61, 363

Steiner, O. 2005, A&A, 430, 691

Title, A. M., Rosenberg, W. J. 1981, Optical Engineering, 20, 815

van Noort, M., Rouppe van der Voort, L. & Löfdahl, M. G. 2005, Solar Physics, 228, 191

Vögler, A., & Schüssler, M. 2003, AN ,324, 399V

Vögler, A.; Shelyag, S.; Schüssler, M.; Cattaneo, F.; Emonet, T.; Linde, T. 2005, A&A, 429, 335